

# A Comparison of Separated Flow Airfoil Analysis Methods

John D. Blascovich\*

Grumman Aerospace Corporation, Bethpage, New York

A correlation study is performed to determine the engineering value of several current computational methods which analyze airfoils with separated flow. Three computer codes are used to evaluate six different airfoils at several Mach and Reynolds numbers. The results indicate that no single method is able to analyze both subsonic and transonic trailing-edge separation accurately.

## Nomenclature

$C_D$	= drag coefficient
$C_L$	= lift coefficient
$C_{l_{\alpha_0}}$	= zero angle-of-attack lift curve slope
$C_m$	= moment coefficient calculated about airfoil quarter-chord
$C_p$	= pressure coefficient
$C_3, C_3^*$	= terms used in Barnwell's boundary-layer thickness equation
$q$	= local boundary-layer edge velocity
$RN$	= Reynolds number
$s$	= airfoil arc length
$U_e$	= transformed boundary-layer edge velocity
$U_{e_{sep}}$	= value of $U_e$ at separation point
$SP$	= separation parameter
$X$	= Cartesian chordwise coordinate
$X_{sep}$	= value of $X$ at the separation point
$\alpha$	= angle of attack of airfoil with respect to the freestream
$\delta$	= boundary-layer thickness
$\delta_{sep}$	= boundary-layer thickness at separation point
$\theta$	= local momentum thickness

## Introduction

THE ability to predict the onset of flow separation on a two-dimensional airfoil section is of great value to aerodynamicists. Although separation is not usually a problem during normal cruise conditions, it is of importance for high-lift portions of the flight regime, such as takeoff and landing, and transonic maneuvering. The designer always strives to maximize lift while avoiding the drag penalties incurred by sustaining large regions of separated flow. Since this aspect of wing design is still largely dependent on expensive wind tunnel tests, accurate analysis programs could reduce costs significantly.

Flows with regions of separation are dominated by viscous effects and cannot be analyzed using ordinary inviscid methodology. This greatly increases the complexity of the problem. The existence of different types of separation serves to make matters even worse. Separation can be classified as laminar or turbulent, and leading edge, trailing edge, or shock induced. In general, separation of a boundary layer occurs in regions with an adverse pressure gradient. The low kinetic energy of the fluid particles in the decelerated boundary layer occurs in regions having an adverse pressure gradient. The low kinetic energy of the fluid particles in the decelerated

boundary layer prevents them from penetrating into regions of increased pressure; therefore, the boundary layer is deflected from the surface and separates. The point of separation in two-dimensional flow is defined as the point at which the wall shear stress is equal to zero. The separated zone is characterized by a region of reverse flow, with the rear stagnation point of the flow residing at the rear of the separated bubble. In an unsteady flow, mass is transferred between the bubble and the external flow. At low speeds and high angles of attack, the pressure of the separated zone remains relatively constant.

The goal of this study is to compare several readily available functioning computer programs that model flow separation. The type of separation of interest is mainly the turbulent trailing-edge variety, at both subsonic and transonic speeds. The three codes discussed provide a good example of the range of methods in use today and are available to general users. The three programs are CLMAX, a subsonic panel code developed by Analytical Methods Inc.<sup>1</sup>; TRANSEP, a finite difference method developed by Carlson<sup>2</sup> and Barnwell's<sup>3</sup> subsonic/transonic finite difference code.

Although good data are not plentiful, a search produced reports on six airfoils: the NASA GA(W)-1, NASA GA(W)-2, NACA 65-213, NACA 4412, NACA 0012, and the NASA A-1 rotor airfoil.<sup>4-9</sup> These six airfoils provide a range of thickness, leading-edge radii, camber lines, and technology level (supercritical vs conventional). The data were used to determine each code's ability to predict pressures, forces, and moments for cases involving varying degrees of separated flow.

## Discussion

The complexity of separated flow has made analysis of the problem difficult, which explains the current extensive use of the wind tunnel for determining maximum lift, high angle-of-attack stability, and flow separation visualization. Dozens of methods for analyzing both laminar and turbulent separation have been formulated during the past 50 years, but none have been widely used for analysis purposes. This is partially due to the fact that many methods required numerical solution of the boundary-layer equations, which dictated a formidable number of computations.

The expanded capability of the modern computer is improving this situation. Efforts are currently under way to solve various versions of the Navier-Stokes equations. These range from direct solution of the full unsteady equations to solution of the Reynolds-averaged equations with turbulence modeling. The latter is the focus of almost all current research in the area. Although solution of the Reynolds-averaged equations could provide very accurate results, this may not occur in the near future. A better understanding of the physics of turbulence is required before proper turbulence models can be formulated. There is a need for a simpler yet accurate

Presented as Paper 84-0048 at the AIAA 22nd Aerospace Sciences Meeting, Reno, Nev., Jan. 9-12, 1984; received May 21, 1984; revision received Oct. 19, 1984. Copyright © American Institute of Aeronautics and Astronautics, Inc., 1984. All rights reserved.

\*Associate Engineer, Aerodynamics Section. Member AIAA.

engineering tool to bridge the gap. The programs described below represent contemporary attempts to fill this need.

The codes were executed for a large number of test cases (18 sets of force and moment data, 23 pressure runs). Space limitations prevent all of the cases from appearing below, therefore, a representative subset has been presented.

The methods were run the same way for all airfoils, without adjustments to tailor the results to match the data. Inputs for starting conditions were modified as described in the users' manuals. The airfoil ordinates were obtained from the test reports and all contain sufficient resolution to satisfy the codes used for the effort.

### CLMAX

The CLMAX code, developed by Maskew and Dvorak<sup>1</sup> at Analytical Methods, Inc., is an incompressible vortex panel method designed to calculate the flow around airfoils up to and beyond stall. The potential flow program is coupled to a laminar boundary-layer method, Curle's method,<sup>10</sup> and an integral turbulent boundary-layer method developed by Nash and Hicks.<sup>11</sup> The laminar calculation is performed along the entire airfoil unless transition or separation is found. The turbulent calculation begins at that point, and determines separation when the skin friction goes to zero.

Free vortex sheets are used by the program to construct a wake once separation is found. The shape of the wake is initially prescribed using empirical rules, with the final shape determined iteratively through interaction with the potential flow program. The free vortex sheets are constructed by fitting parabolic curves between the separation points (upper and lower, if found) and a point downstream. The downstream distance of this point is determined using a free parameter called the wake-fineness ratio, which is basically an aspect ratio of the wake.

Convergence criteria for the wake shape iteration and the potential flow iteration have not been investigated thoroughly, therefore, the user has the option of setting these variables. The code does not require large amounts of computer time, achieving solutions in 25-30 sec of CPU time per angle of attack (when run through a series of increasing angles) on an IBM 3033. Required storage is 256 kilobytes.

Runs were made using the Nash-Hicks boundary layer, with six viscous/potential flow iterations and two wake shape iterations. In general, the program was fairly simple to operate. A series of increasing angles of attack were usually run, with the separation points from the lower angles used as initial data for the higher ones. This is the most efficient way to run the program, and the results are generally the same as those obtained running one angle of attack at a time.

The most important variables to the solution accuracy are the number of wake shape iterations, the wake fineness ratio, and whether or not transition is specified. The number of wake iterations used for the cases shown herein was two. Initially, three were tried, as recommended in Ref. 1, but the results obtained did not match those in the reference. The wake fineness ratio curve was probably correlated using two wake iterations, and it may have to be adjusted if the user wants to run three iterations. Using two wake iterations and the wake fineness ratios obtained from the aforementioned reference produced the best results. The option of fixing transition vs not specifying it was exercised on several cases. On the upper surface of the airfoil, especially at high angles of incidence, very minor differences were noted, since the laminar boundary layer usually separated very close to the leading edge for both cases, before the fixed transition point. On the lower surface, the boundary layer is laminar for at least 40% of the airfoil, to avoid having the transition point coincide with the stagnation point. If transition was not specified, the laminar run was generally 10% longer than that allowed when transition was fixed. Fixing transition sometimes caused significant (and unrealistic) changes in the

lift curve. For this reason, the code should be run without fixing transition.

The number of panels used in the calculations was between 75 and 80. Although extensive tests were not conducted, several runs using 50-60 panels were tried, producing poor results. When the preceding guidelines were followed, CLMAX proved to be relatively straightforward to use.

Pressure comparisons are shown for two airfoils to illustrate typical results. Figure 1 shows the 17%-thick GA(W)-1 at a Mach number of 0.15, a Reynolds number of  $6.3 \times 10^6$ , and angle of attack of 18.25 deg. The code shows excellent agreement with data. Figure 2 shows a comparison for the NASA A-1 rotor airfoil at a Mach number of 0.30 and an angle of attack of 14 deg. In this case, the flow has separated at the leading edge, which the code cannot predict accurately. A laminar leading-edge separation predictor would be needed to analyze this case properly.

### Barnwell

Barnwell's potential flow/boundary method<sup>3</sup> utilizes a finite difference transonic potential flow method and a moment-of-momentum integral boundary-layer calculation. The potential flow method evaluates the exact boundary condition slope on the airfoil chord line. This allows the use of a simple nonuniform Cartesian grid instead of a more complex mapping scheme. The flow equation is solved using line relaxation. The integral boundary-layer method is a simplification of the method of Kuhn and Nielsen<sup>12</sup> which itself is a modification of the Nash and Hicks<sup>11</sup> routine used in the CLMAX code. This method is intended to model both subsonic and transonic trailing-edge separation.

The boundary-layer algorithm solves the momentum equation, the moment-of-momentum equation, and a boundary-layer edge condition. The integral mean kinetic energy equation can be solved as an alternative to the moment-of-momentum equation. Laminar sublayers are ignored because of numerical considerations. Once separation is found, the program evaluates boundary-layer thickness  $\delta$  using the closed-form solution

$$\delta = \delta_{sep} [1 + C_3^* (X - X_{sep})] \quad (1)$$

where

$$C_3^* = \frac{48\pi^2 C_3}{(5\pi^2 - 32)\delta_{sep}} \quad \text{and } C_3 = \text{const}$$

Velocity (pressure) in the separated region can vary as

$$U_e = \frac{U_{e_{sep}}}{[1 + C_3^* (X - X_{sep})]^{1/6}} \quad (2)$$

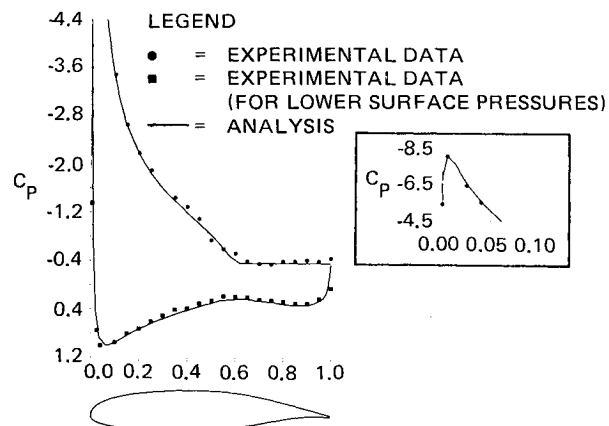


Fig. 1 Chordwise pressure distribution, GA(W)-1 Airfoil:  $M=0.15$ ,  $\alpha=18$  deg,  $RN=6.3 \times 10^6$ .

or it can be set constant throughout. Drag is computed using a Squire-Young approximation based on the wetted area.

The potential flow method supplies Neumann boundary conditions on the attached-flow portion of the airfoil, and switches to Dirichlet boundary conditions on the separated region. The governing equation is a modification of the small-disturbance equations containing additional terms selected by Barnwell from the full potential equation.

The program was under development during this study, and had many options available to the user. A certain amount of empiricism is present in the code. The first is the option to specify constant pressure in the separated zone, which is widely accepted for subsonic flow. The second is the dependence of the solution on the initial attached potential flow (or starting) solution. Acceptable results are best achieved when the angle of attack of the starting solution is 3-4 deg lower than that of the desired solution. Both of these angles must be specified as program input parameters.

During the course of the survey, an error was detected in the moment calculation performed by the program. This was corrected and checked on two of the test cases that appear in the results section. Moment results for the other airfoils and conditions are not shown, since time constraints precluded rerunning all of the cases.

Once the effects of the different parameters mentioned previously were sorted out, the code proved relatively easy to use. All cases shown in this paper, unless otherwise noted, were run in the following manner. The angle of attack of the starting solution (ALPHAS) was 3 deg lower than that of the actual angle of attack (ALPHAD). The nonconservation form was always chosen (IDIF=1) as was the constant-pressure approximation after separation (ASRIF=0). Lower surface transition was set at an  $X$  index of 36 ( $X/C=0.31$ ) to prevent any interference with the stagnation point at large incidence angles. Upper surface transition was set at the leading edge, since there are cases for which a shock wave occurs close to the leading edge. If the shock occurs before transition, no shock-wave/boundary-layer interaction can occur and the results will be inaccurate. The moment-of-momentum equation was used. Finally, the grid system supplied with the code was used for all of the cases although it required some modification for the GA(W)-1, as will be noted shortly. The grid was not halved in the  $X$  direction, but was halved once in the  $Z$  direction to allow faster convergence on the coarse grid. The grid is input as part of the data set.

The code was relatively easy to use when run as noted previously producing, generally good results. Convergence usually was not a problem, and changing the PHI-XT damping parameter (EPSI) from 0 to 1 solved any difficulties that were encountered. Although the program can be run through a series of increasing angles of attack, the use of this option produced results which differed significantly from single angle of attack runs. Therefore, the code should be executed once for each angle of attack. The program requires about 5 min of CPU time and 77,231 octal words of storage on a CDC CYBER 740 machine.

Figures 3 and 4 present the sample pressure distributions for the GA(W)-1 and A-1 airfoils. The code performs fairly well on the GA(W)-1, missing the pressure level in the separated zone due to the lack of a wake model. The A-1 case exhibits the same shortcoming, in addition to showing the need for laminar separation prediction.

### TRANSEP

TRANSEP, developed by Carlson,<sup>2</sup> is a modified version of the earlier transonic TRANDES code. Addition of a separation modeling scheme allows this newer program to analyze airfoils in subsonic flow with regions of massive separation.

The program utilizes a finite difference full potential code coupled with a Thwaites laminar boundary-layer routine and a Nash-McDonald integral turbulent boundary-layer method.

The potential flow code solves the exact perturbation potential equation iteratively using rotated finite differences and column relaxation. A Cartesian grid system is used to model the airfoil. The program will initially solve the flow on a  $7 \times 13$  grid as a default, and will halve the grid as directed by the user. The medium grid (NHALF=2) is  $49 \times 25$ , while the fine grid (NHALF=3) is  $97 \times 49$ .

The separation point is calculated in the Nash-McDonald routine, using the parameter called SEP, which is defined as:

$$SEP = -\frac{\theta}{q} \frac{dq}{ds}$$

When SEP exceeds a specific value,  $SP$ , separation is assumed to occur. The  $SP$  parameter is calculated using empirical equations which are functions of angle of attack, Reynolds number, and low angle of attack lift curve slope.

When separation is located, the separated pressure is calculated using the velocity potentials at the trailing edge and at separation, and the length of the separated region. The pressure in the entire separated zone is set to this value, and the potential flow code uses inverse boundary conditions to calculate a displacement surface. Drag is calculated using a Squire-Young approximation evaluated at separation, but using the distance to separation as the reference length.

The code requires approximately 4 min of CPU time running on the fine grid for one angle of attack, and under 300 kilobytes of storage on an IBM 3033.

TRANSEP proved relatively easy to use, but it could not successfully run the full set of test cases. All cases above a

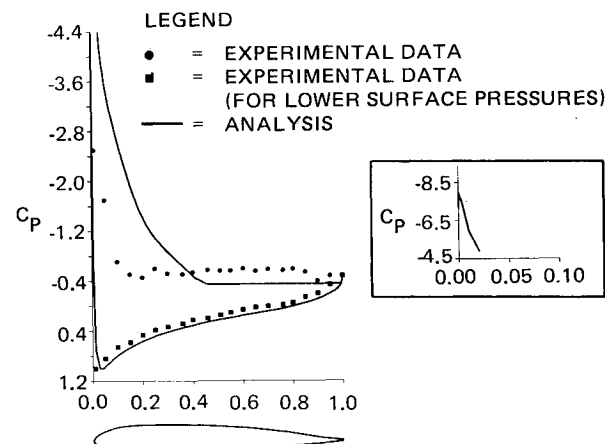


Fig. 2 Chordwise pressure distribution, NASA A-1 Airfoil:  $M=0.30$ ,  $\alpha=14$  deg,  $RN=2.5 \times 10^6$ .

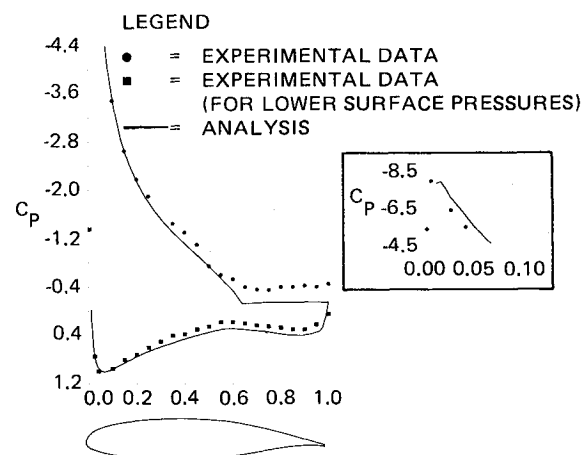


Fig. 3 Chordwise pressure distribution, GA(W)-1 Airfoil:  $M=0.15$ ,  $\alpha=18$  deg,  $RN=6.3 \times 10^6$ .

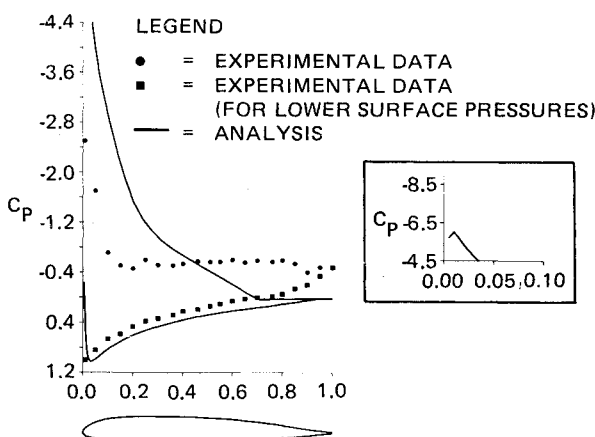


Fig. 4 Chordwise pressure distribution, NASA A-1 Airfoil:  $M=0.30$ ,  $\alpha=14$  deg,  $RN=2.5 \times 10^6$ .

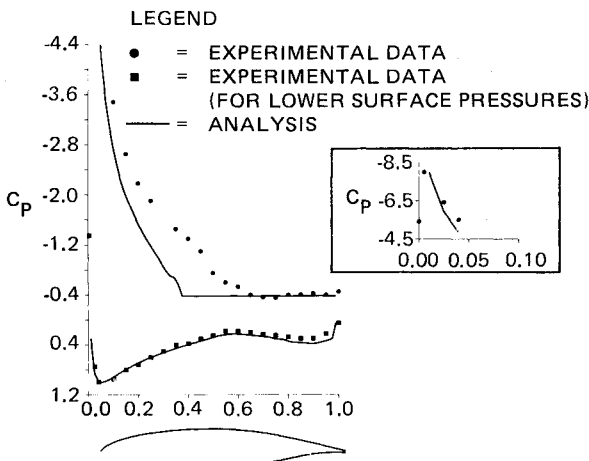


Fig. 5 Chordwise pressure distribution, GA(W)-1 Airfoil:  $M=0.15$ ,  $\alpha=18$  deg,  $RN=6.3 \times 10^6$ .

Mach number of 0.30 would incur numerical errors at angles of attack lower than the stall angle. This is due, in part, to the fact that the massive separation methodology and constant-pressure approximation are not valid for transonic flow, which can occur at high angles of attack at Mach numbers as low as 0.30. There are also difficulties related to the empirical formulas which specify the separation parameter,  $SP$ . For angles of attack greater than 15.3 deg the following formula, which is suggested by Carlson, is used:

$$SP = 3.6213784 \times 10^{-3} + 0.0142875 C_{l_{\alpha_0}} + (-8.4074 \times 10^{-11} RN + 2.1707 \times 10^{-4}) (\alpha - 15.3)$$

As the angle of attack increases,  $SP$  should decrease since separation is more likely to occur. This will be the case as long as the Reynolds number is greater than  $2.58 \times 10^6$ , since the term containing  $RN$  will be negative and grow as the angle of attack grows. However, for Reynolds numbers below  $2.58 \times 10^6$ , the term will become positive and  $SP$  will grow with increasing angle of attack. This will prevent the separation point from moving forward, and stall will not be found. If the stall of the airfoil is calculated before 15.3 deg, this will not be a problem since the formula used for that case does not have a Reynolds number term in it. Of course, the user can modify the formula if low Reynolds number cases are of interest, but there was insufficient time during this effort to determine the best way to do this.

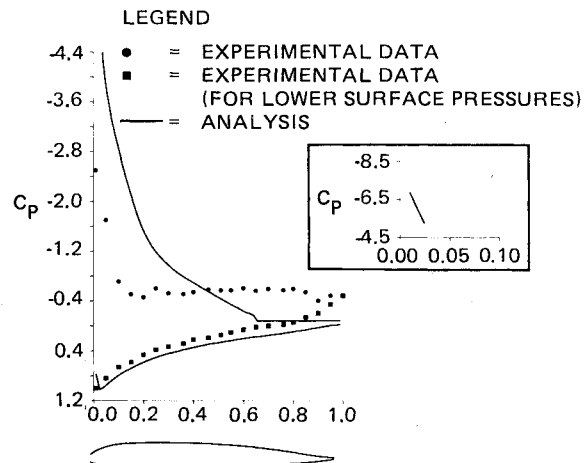


Fig. 6 Chordwise pressure distribution, NASA A-1 Airfoil:  $M=0.30$ ,  $\alpha=14$  deg,  $RN=2.5 \times 10^6$ .

The runs used herein observed the following conventions. The  $C_L$  calculated by pressure integration was used instead of that calculated using the circulation around the airfoil (CLCIR). The massive separation parameter (IMASS), which allows the separation search to take place, was set to enable the search (IMASS = 1). Running the code this way has the effect of forcing separation even at low angles of attack, which causes poor correlations at those angles. This is a consequence of the relatively simple separation point prediction used in the code.

The program will produce better correlations at low angles of attack if IMASS is set to zero, as the user's manual states. This was not done for this study since such correlations were not the focus of this effort.

The pressure comparisons for this code illustrate some of the above points. The GA(W)-1 case (Fig. 5) shows that the inaccuracy of the separation point prediction is the main difficulty for the code in this case. The lack of a leading-edge criteria, shared by other codes in this study, explains the results for the A-1 airfoil (Fig. 6).

### Code vs Code Comparisons

The best way to illustrate the relative strengths of the programs is to superimpose the results on the same plot. The GA(W)-1 at a Reynolds number of  $6 \times 10^6$  is shown in Fig. 7. Both CLMAX and BARNWELL perform very well. The CLMAX results are from the transition-free run. CLMAX has a slightly better drag prediction, although neither is particularly good. At a Reynolds number of  $2.1 \times 10^6$  (Fig. 8), both BARNWELL and CLMAX overpredict the angle and value of maximum lift, but TRANSEP is very close to the correct values. CLMAX shows the best drag results, although more data at higher lift would be desirable for a better check of code accuracy.

Comparisons for the GA(W)-2 test cases are plotted in Figs. 9 and 10. The higher Reynolds number results (Fig. 9) show CLMAX, BARNWELL, and TRANSEP predicting very good maximum lift and stall angle values. TRANSEP, with its modified Squire-Young predictor, yields the best drag results. Lower Reynolds number results (Fig. 10) show none of the codes closely matching the data. The CLMAX code with transition would match the data, but it seems to be more consistent running with transition unspecified, so that is what is presented here. TRANSEP cannot handle the low Reynolds number case because of the  $SP$  calculation equation above 15.3 deg. CLMAX exhibits the best drag results but without a good lift prediction, therefore, these are not of great value.

The NACA 4412 results (Fig. 11) show TRANSEP predicting an accurate value of maximum lift at the correct

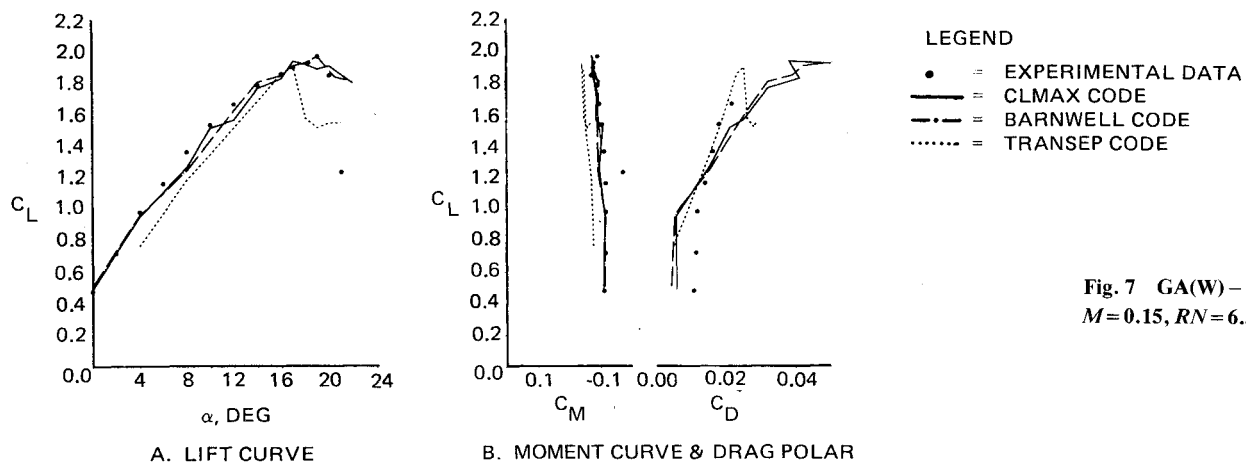


Fig. 7 GA(W)-1 Airfoil:  
 $M=0.15$ ,  $RN=6.3 \times 10^6$ .

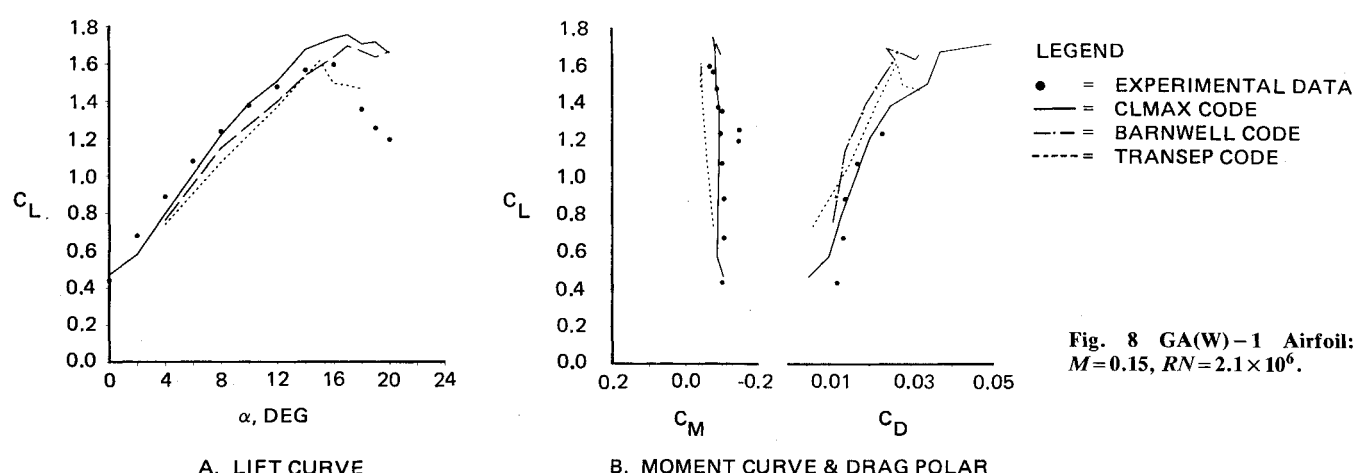


Fig. 8 GA(W)-1 Airfoil:  
 $M=0.15$ ,  $RN=2.1 \times 10^6$ .

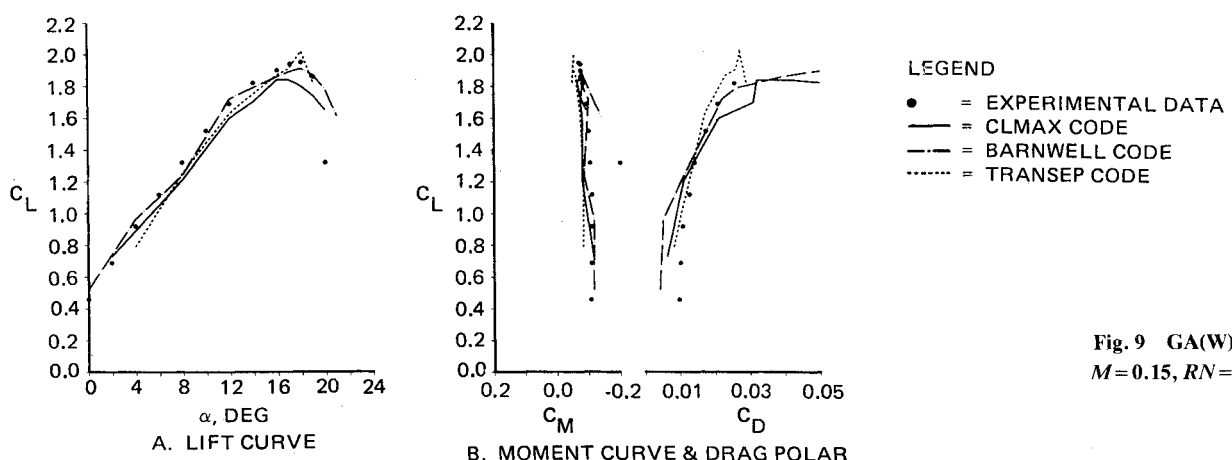


Fig. 9 GA(W)-2 Airfoil:  
 $M=0.15$ ,  $RN=4.3 \times 10^6$ .

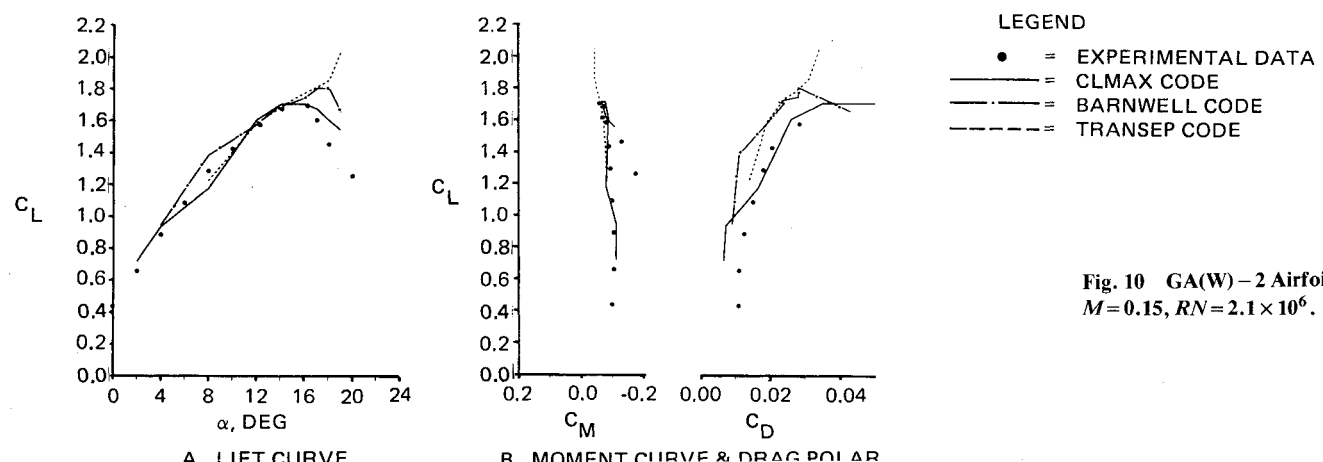
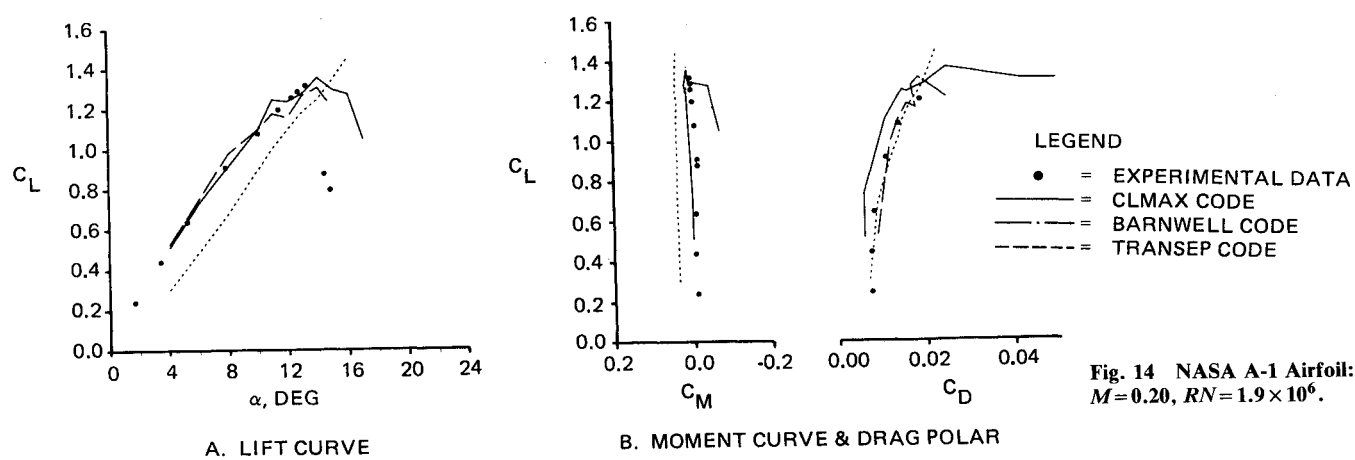
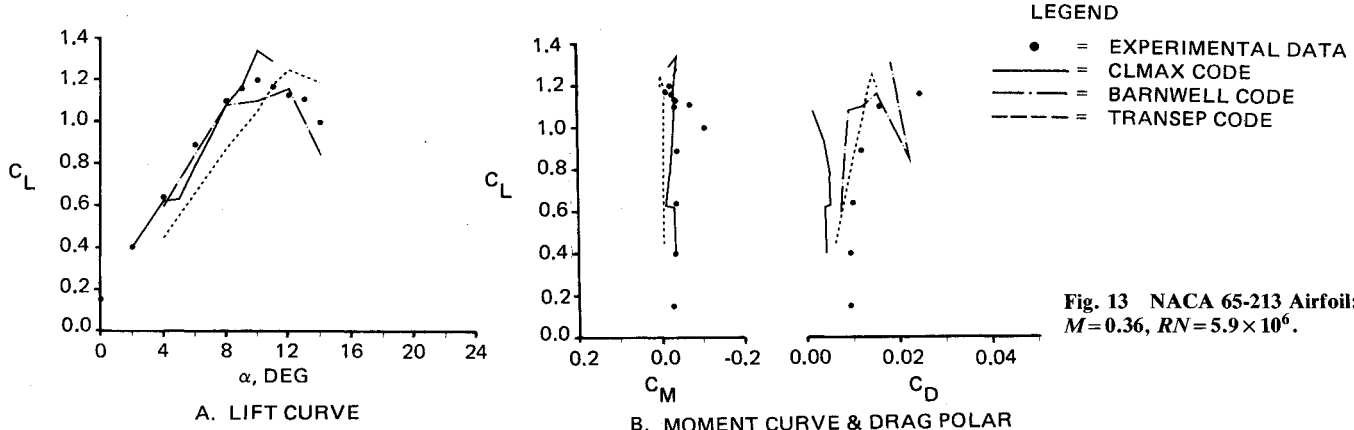
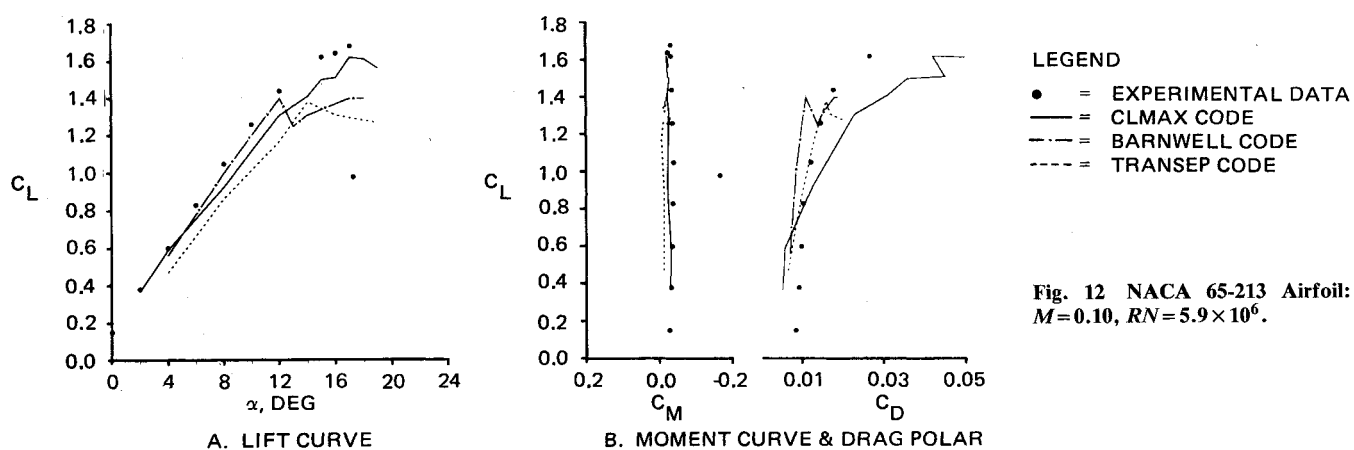
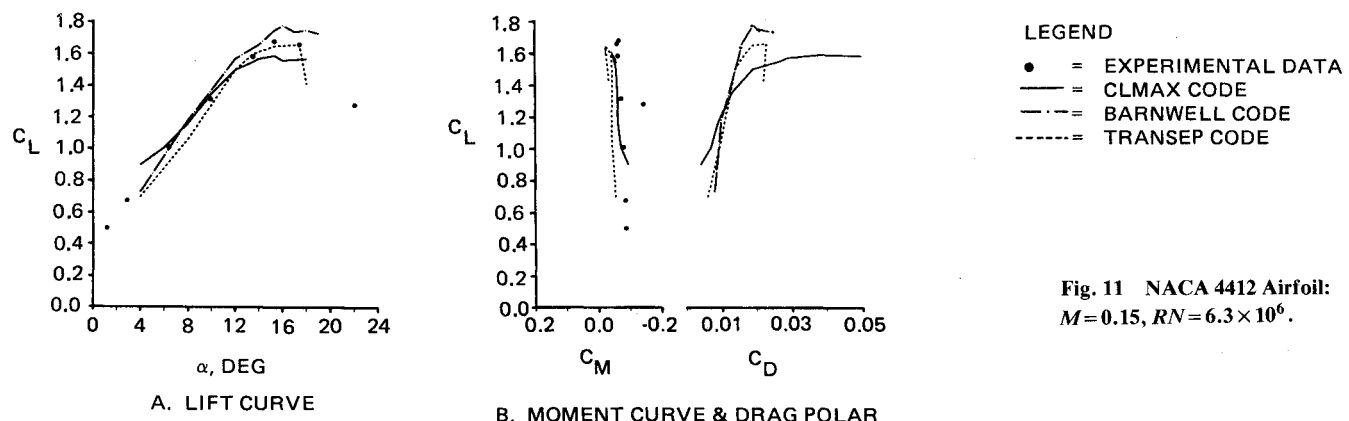


Fig. 10 GA(W)-2 Airfoil:  
 $M=0.15$ ,  $RN=2.1 \times 10^6$ .



angle, with BARNWELL and CLMAX yielding the correct angle, but giving maximum lift values which are not very close. TRANSEP's good correlation is not surprising, since the *SP* calculation formulas were created using the airfoil as one of the test cases. Since drag data were not available drag comparisons are meaningless.

The NACA 65-213, perhaps the most difficult test case, illustrates the drawbacks caused by using planar boundary conditions and a Cartesian grid. At a Mach number of 0.10 (Fig. 12), only CLMAX produces a lift curve which is close to the data. The poor showings of both TRANSEP and BARNWELL are probably due to the small leading-edge radius of the airfoil.

The results at a Mach number of 0.36 (Fig. 13) show none of the codes predicting both stall angle and maximum lift correctly. BARNWELL predicts the best value of maximum lift, but CLMAX calculates the proper stall angle. Since compressibility is important in this case, CLMAX should not do very well as indicated by the drag prediction. The experimental lift curve for this case indicates that the stall is more gradual than at the lower Mach number cases. Since leading-edge separation is not present, the Cartesian codes are able to perform better for this case than for the others.

No single code functions well through the entire range of conditions for this particular airfoil. CLMAX does the best most often, but it is not very good. This is due in part to the lack of a laminar separation predictor for any of the codes, and to the problems posed at the leading edge when using a Cartesian grid system to model airfoils with small nose radii.

The A-1 airfoil also exhibits a stall characterized by leading-edge separation at low Mach numbers. It also provides a difficult test case. The results for a Mach number of 0.20 at a Reynolds number of  $1.9 \times 10^6$  are seen in Fig. 14.

CLMAX and BARNWELL both predict accurate values of maximum lift and stall angle. TRANSEP fails to predict a turnover in the lift curve, due to the limitations of the *SP* calculation which was in the code. Both BARNWELL and TRANSEP produce good drag correlations for lift coefficients up to the maximum for which drag data were obtained.

The next case was for a Mach number of 0.50 (Fig. 15). BARNWELL and CLMAX both yield usable stall angle and maximum lift predictions, while TRANSEP fails to run above 8 deg. However, while BARNWELL predicts minimal separation until the maximum lift point, CLMAX is showing significant separation at 6-deg angle of attack. Therefore, the good agreement with data may be coincidental, and the pressure data from the code must be disregarded.

The moment prediction by CLMAX shows the region where the separated flow causes a positive shift in the curve which is not present in the data. None of the codes predicts the drag adequately through the highest lift levels.

The NACA 0012, another airfoil exhibiting leading-edge stall at low Mach numbers, is covered in Figs. 16 and 17. At a Reynolds number of  $6 \times 10^6$  and a Mach number of 0.15 (Fig. 16), TRANSEP showed the best value of both maximum lift and stall angle, while BARNWELL produced excellent agreement with data at lower angles with an early stall prediction. CLMAX did not do very well for this case. TRANSEP also managed the best drag correlation, although its poor performance along the attached-flow portion of the lift curve makes this correlation very questionable.

At the higher Mach number of 0.55, BARNWELL calculates the most consistent results. Figure 17 illustrates the comparison at a Reynolds number of  $3 \times 10^6$ , with Barnwell and CLMAX yielding usable lift curves. TRANSEP would

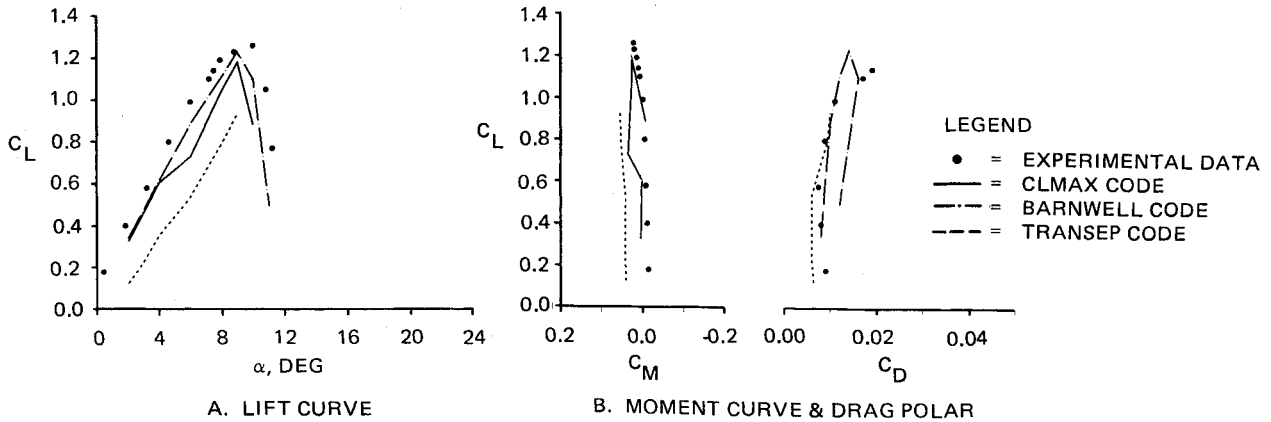


Fig. 15 NASA A-1 Airfoil:  $M=0.50$ ,  $RN=3.5 \times 10^6$ .

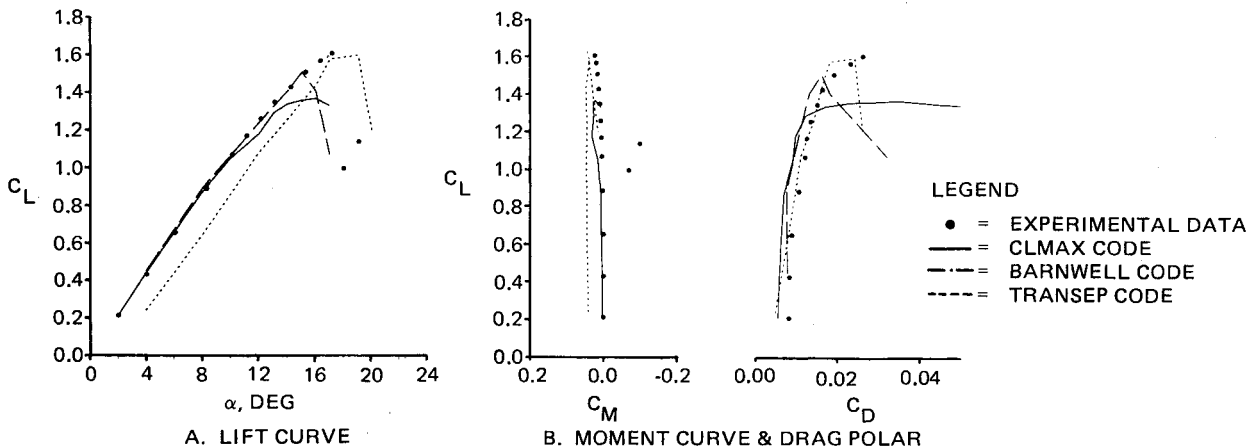
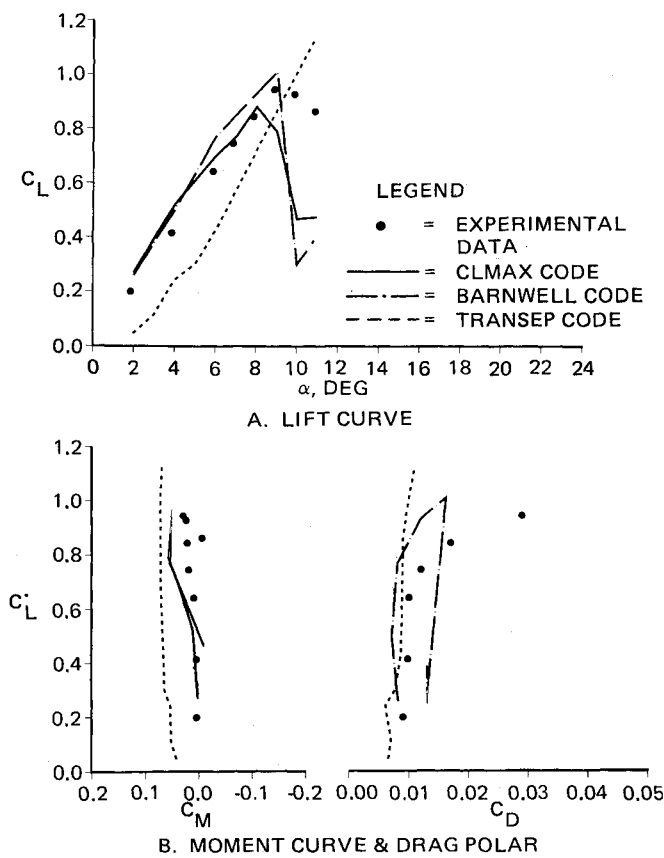


Fig. 16 NACA 0012 Airfoil:  $M=0.15$ ,  $RN=6 \times 10^6$ .

Fig. 17 NACA 0012 Airfoil:  $M=0.55$ ,  $RN=3\times 10^6$ .

not run past 10.8 deg due to numerical instabilities. The moment and drag results are not very encouraging for any of the codes due to the general difficulty in calculating drag, especially for cases with both transonic effects and separation present. Note that the experimental data for this Mach number are uncorrected, which is why the codes predict higher lift slopes than the data.

### Concluding Remarks

The purpose of this effort was to evaluate several methods of analyzing airfoils featuring flow separation with an emphasis on the engineering utility of each. Most of the codes tested could be "fine tuned" for each airfoil and thereby produce better results than some included here, but this requires experimental data for the airfoil in question. This luxury is not available to the designer during initial design phases, therefore, the analysis code must be capable of yielding good results without the user knowing the answer beforehand.

The CLMAX code is very good for analyzing low-speed, high-angle-of-attack cases. The method will yield reasonable values of maximum lift and stall angle for most cases when using the parameters noted in this study. Strengths of the program include ease of operation, low CPU requirements, and multiple angle-of-attack capability. Weaknesses of the code are the lack of a laminar separation criteria and its inability to handle cases with strong compressibility effects.

The BARNWELL method performed well on cases with significant compressibility effects. Good results were also obtained for low-speed cases on airfoils without sharp leading edges. The constant separated pressure used herein produces more consistent results than the variable-pressure option. The weaknesses of this code are related to the Cartesian grid and

planar boundary conditions used for geometry modeling, and the absence of a wake model. Finally, the dependence of the solution on the starting conditions is somewhat awkward.

The TRANSEP program produced good results for several airfoils but is difficult to use as an engineering tool. The separation point predictor in the turbulent boundary-layer routine is very empirical, as noted in Ref. 4. Modification of the equation used to calculate the separation parameter can be difficult when analyzing new airfoils without prior wind tunnel tests. TRANSEP is well suited for subsonic analysis of families of airfoils which include at least one "known" case with experimental data.

The results of this effort show that no single method was able to accurately analyze a series of airfoils, treated as unknowns, through both subsonic and transonic speeds. The keys to predicting separated flowfields are accurate separation point prediction and proper accounting of the wake region. Improvements in these areas will be crucial to the advance of the state-of-the-art.

### Acknowledgments

This work was performed as a cooperative effort in partial fulfillment of the requirements for the degree of Master of Science (M.I.T.). The author wishes to acknowledge the efforts of Prof. Earll Murman at M.I.T., who served as Thesis Advisor for this effort and provided invaluable assistance. Thanks are also due to Charles Boppe at Grumman Aerospace, who served as Company Supervisor.

### References

- 1 Maskew, B. and Dvorak, F. A., "Investigation of Separation Models for the Prediction of  $C_L$  MAX," AHS Paper 77-33-01, May 1977.
- 2 Carlson, L.A., "TRANSEP: A Program for High Lift Separated Flow About Airfoils," NASA CR-3376, Dec. 1980.
- 3 Barnwell, R. W., "A Potential Flow/Boundary Layer Method for Calculating Subsonic and Transonic Airfoil Flow with Trailing-Edge Separation," NASA TM-81850, June 1981.
- 4 McGhee, R. J. and Beasley, W. D., "Low-Speed Aerodynamic Characteristics of a 17-Percent-Thick Airfoil Section Designed for General Aviation Applications," NASA TN D-7428, Dec. 1973.
- 5 McGhee, R. J., Beasley, W. D., and Comers, D. M., "Low-Speed Aerodynamic Characteristics of a 13-Percent Thick Airfoil Section Designed for General Aviation Applications," NASA TM-X 72697, May 1977.
- 6 Pinkerton, R. M., "The Variation with Reynolds Number of Pressure Distribution Over an Airfoil Section," NACA Rept. 613, 1938.
- 7 Beasley, W. D. and McGhee, R. J., "Experimental and Theoretical Low-Speed Aerodynamic Characteristics of the NACA 65-213,  $\alpha=0.50$ , Airfoil," NASA TM X-3160, Feb. 1975.
- 8 Hicks, R. M. and McCroskey, W. J., "An Experimental Evaluation of a Helicopter Rotor Section Designed by Numerical Optimization," NASA TM-78622, March 1980.
- 9 Harris, C. D., "Two-Dimensional Aerodynamic Characteristics of the NACA 0012 Airfoil in the Langley 8-Foot Transonic Pressure Tunnel," NASA TM-81927, April 1981.
- 10 Curle, H., "A Two-Parameter Method for Calculating the Two-Dimensional Incompressible Laminar Boundary Layer," *Journal of the Royal Aeronautical Society*, Vol. 71, February 1967, pp. 117-123.
- 11 Nash, J. F. and Hicks, J. G., "An Integral Method Including the Effect of Upstream History on the Turbulent Shear Stress," *Computation of Turbulent Boundary Layers-1968 AFOSR-IFP-Stanford Conference, Vol. I-Methods, Predictions, Evaluation and Flow Structure*, edited by S. J. Kline, M. V. Morkovin, G. Sovran, and D. J. Cockrell, Stanford University, Calif., 1969, pp. 37-45.
- 12 Kuhn, G. D. and Nielsen, J. N., "Prediction of Turbulent Separated Boundary Layers," AIAA Paper 73-663, July 1973.